DMD Fast Forward. Published on November 8, 2005 as doi:10.1124/dmd.105.007112
This article has not been copyedited and formatted. The final version may differ from this version.

Characterization of the *In vitro* Metabolism of Selective Androgen Receptor Modulator (SARM) Using Human, Rat and Dog Liver Enzyme Preparations

Wenqing Gao, Zengru Wu, Casey E. Bohl, Jun Yang, Duane D. Miller, and James T. Dalton

Division of Pharmaceutics, College of Pharmacy, The Ohio State University, Columbus, OH (W.G., Z.W., C.E.B., J.Y., J.T.D.); Department of Pharmaceutical Sciences, The University of Tennessee Health Science Center, Memphis, TN (D.D.M.)

RUNNING TITLE: Selective Androgen Receptor Modulators

CORRESPONDING AUTHOR: James T. Dalton

ADDRESS: 500 West 12th Avenue

L.M. Parks Hall, Room 242

Columbus, OH 43210

TELEPHONE: 614-688-3797

FAX: 614-292-7766

E-MAIL: DALTON.1@OSU.EDU

NUMBER OF TEXT PAGES: 14

NUMBER OF TABLES: 0

NUMBER OF FIGURES: 9

NUMBER OF REFERENCES: 17

NUMBER OF WORDS: Abstract: 226

Introduction: 575

Discussion: 1333

ABBREVIATIONS: SARM(s), selective androgen receptor modulator(s); AR, androgen receptor(s); HPLC, high-performance liquid chromatography; NAT, N-acetyltransferase; NADPH, nicotinamide adenine dinucleotide phosphate, reduced form; CYP, cytochrome P450; HLM, human liver microsome; ESI, electrospray ionization; MS, mass spectrometry.

ABSTRACT

Compound S4 is a novel nonsteroidal selective androgen receptor modulator (SARM) that demonstrates tissue-selective androgenic and anabolic effects. The purpose of this *in vitro* study was to identify the phase I metabolites, potential species differences in metabolism, and the cytochrome P450s (CYPs) involved in the phase I metabolism of S4 using ^{14}C-S4, recombinant CYPs and other liver enzyme preparations from human, rat, and dog. The major phase I metabolism pathways of S4 in humans were identified as: deacetylation of the B-ring acetamide group, hydrolysis of the amide bond, reduction of the A-ring nitro group, and oxidation of the aromatic rings, with deacetylation being the predominant pathway observed with most of the enzyme preparations tested. Among the major human CYP enzymes tested, CYP3A4 appeared to be one of the major phase I enzymes that could be responsible for the phase I metabolism of S4 (K_m=16.1 μM, V_{max}=1.6 pmole/(pmole·min)) in human, and mainly catalyzed the deacetylation, hydrolysis, and oxidation of S4. In human, the cytosolic enzymes mainly catalyzed the hydrolysis reaction, while the microsomal enzymes primarily catalyzed the deacetylation reactions. Similar phase I metabolic profiles were observed in rats and dogs as well, except for that amide bond hydrolysis seemed to occur more rapidly in rats. In summary, these results showed that the major phase I reaction of S4 in human, rat, and dog is acetamide group deacetylation.

INTRODUCTION

Selective androgen receptor modulators (SARMs) have been proposed as a new class of androgen receptor (AR) ligands with unique tissue selectivity that could be used as safer and more beneficial treatment in male hormone replacement therapy (Negro-Vilar, 1999). Structural modifications of the non-steroidal AR ligand, bicalutamide, turned this 'pure antagonist' into a new series of AR agonist (Dalton et al., 1998). As shown in our previous studies (He et al., 2002; Yin et al., 2003b), the thio linkage and B-ring substitution are critical structural features required for the agonist activity of the ligand. Although it's not clear how the structural modifications affect the ligand receptor interaction, the modifications did significantly change the metabolic profile of the ligands.

The initial change of the B-ring substitution from fluoro group to acetamide group, and the sulfonyl linkage to thio group, greatly improved the binding affinity and *in vitro* agonist activity of acetothiolutamide (Yin et al., 2003c). However, it also made the molecule more susceptible to metabolism, resulting in a short half life (less than one hour in rat) and loss of *in vivo* pharmacological activity. Further modification changed the thio linkage to an ether linkage (compound S4, S-3-(4-acetylamino-phenoxy)-2-hydroxy-2-methyl-N-(4-nitro-3-trifluoromethyl-phenyl)-propionamide) (Yin et al., 2003a), which maintained the agonist activity of the ligand and increased the *in vivo* half life to 3-4 hours in rat (Kearbey et al., 2004). Even so, the ideal half life required for once a day administration of SARM, as proposed by Negro-Vilar, is yet to be achieved. Better understanding of the hepatic metabolism profile of S4 will be helpful to guide additional structural modification.

Our previous studies (Gao et al., 2004) have shown that S4 could not be metabolized in AR target tissues by either 5α-reductase or aromatase. However, the formation of active metabolites *in vivo* represents another possible mechanism for the observed tissue selectivity of SARMs (Yin et al., 2003a). As a matter of fact, the pharmacological activity of another non-steroidal AR antagonist, flutamide, is mediated by its active metabolite, hydroxyflutamide (Katchen and Buxbaum, 1975) (Figure 1). Although S4 is not a substrate for either 5α-reductase or aromatase, it is unclear whether any active hepatic

metabolite(s) could contribute to the pharmacologic activity of S4. The studies described herein were designed to address these issues.

Both flutamide and bicalutamide are structural analogs of S4. The metabolic profiles of flutamide and bicalutamide have been well characterized (Katchen and Buxbaum, 1975; Boyle et al., 1993; McKillop et al., 1993). Hydrolysis of the amide bond and oxidation of the aromatic rings are the major phase I metabolism pathways for both flutamide and bicalutamide (Figure 1). Species differences were observed in bicalutamide metabolism (Boyle et al., 1993; McKillop et al., 1993) (Figure 1 B). Hydrolysis of the amide bond of bicalutamide was only observed in rats, but not in humans and dogs; which explains the prolonged half life of bicalutamide in human (McKillop et al., 1993). In comparison, although the previous compound (Yin et al., 2003c), acetothiolutamide, also undergoes extensive oxidation of the thio group and aromatic rings in rat, amide bond hydrolysis was not observed. Modification of the thio linkage in acetothiolutamide to the ether linkage in S4 was intended to eliminate the possibility of linker oxidation, while maintaining the stability of the amide bond.

In current study, the metabolic profile and potential species differences in the metabolism of S4 were characterized using recombinant human cytochrome P450 (CYP) enzymes and pooled liver enzyme preparations from rats, dogs and humans.

MATERIALS AND METHODS

Materials

Compounds S4 and M1, and ^{14}C-S4 were synthesized in our laboratories. Recombinant human CYP enzyme and insect cell control (Supersome®), pooled human, rat, and dog liver microsome, cytosol, and S9 preparations were purchased from BD Gentest (Woburn, MA). 4'-Hydroxy-diclofenac, 4'-hydroxy-mephenytoin, mephenytoin, 1'-hydroxy-bufuralol, and bufuralol were also purchased from BD Gentest. EcoLite™(+) scintillation cocktail was purchased from ICN Research Products Division (Costa Mesa, CA). All other chemicals and reagents were purchased from Sigma Chemical Company (St Louis,

MO). All analytical columns were purchased from Waters Corporation (Milford, MA). NHS-Biotin (N-hydroxysuccinimidobiotin) was purchased from PIERCE (Rockford, IL).

In Vitro Metabolism Reactions

In vitro enzyme reactions were conducted according to the instructions provided by BD Gentest. All phase I reactions were conducted at 37°C in the presence of 1 mM NADPH (Nicotinamide adenine dinucleotide phosphate, reduced form) in 100 mM phosphate buffer (pH 7.4) for various times. For liver microsomes, cytosol, or liver S9 preparations, total protein concentration of 2 mg/ml was used in the reaction, and the recombinant CYP enzymes were used with the final concentration of 200 pmole/ml. In general, the incubation time was 2 hours for metabolite identification, while incubation time for the determination of enzyme kinetics parameters was 10 minutes. Incubation conditions were optimized so that the rate of metabolism was linear with respect to incubation time and microsomal protein concentration. The kinetic parameters, Km and Vmax, were determined by nonlinear regression analysis using WinNonlin (version 4.0, Pharsight Corporation, Mountain View, CA) and the Michaelis-Menten kinetics model. For experiments using recombinant CYP enzymes, insect cell control Supersome® was included as a control for native activities from the expression system, and comparable protein concentrations were used. Reactions were stopped by adding ice-cold acetonitrile (v:v/1:1) containing internal standard (CM-II-87, a structural analog of S4) for HPLC analysis. Protein present in the reaction mixture was precipitated by centrifugation (> 16,000 g, 30 min at 4°C), and the supernatant was either diluted with appropriate mobile phase or directly used for HPLC analysis. S4 was separated on a reversed-phase column (Symmetry® C8, 3.9 × 150 mm) with a mobile phase of 45% acetonitrile and 50 mM phosphate buffer (pH 4.8) in deionized water, at a flow rate of 1.0 ml/min, and was detected by its UV absorbance at 230 nm.

Identification of the Phase I Metabolite of S4

^{14}C-S4 (2 μM) was incubated with human, rat, or dog liver preparations at 37°C for 2 hours. After precipitation of the protein with acetonitrile (v:v/1:1), the organic phase left in the supernatant was evaporated under nitrogen, and the resulting concentrated samples were used for HPLC analysis. ^{14}C-S4

and its metabolites were separated using a reversed-phase column (NovaPak C18, 3.0 × 300 mm) with a mobile phase of acetonitrile in deionized water at a flow rate of 1 ml/min. The initial mobile phase contained 0% acetonitrile and was maintained at this composition for 3 minutes. The percentage of acetonitrile was increased to 5% linearly over the next 7 minutes, and was further increased to 30% in the following 5 minutes. The percentage of acetonitrile was again slowly increased to 35% over the next 15 minutes, then rapidly changed to 95% in another 5 minutes, and was maintained at this composition for 5 minutes. Finally, the percentage of acetonitrile was returned to 0% in the last 5 minutes. The eluted fractions (30 seconds per fraction) from the HPLC were collected, and the total radioactivity (DPM) in each fraction was counted in EcoLite™(+) scintillation cocktail.

A similar experiment was conducted using non-radiolabeled S4. In this case, the eluted fractions containing possible metabolites were analyzed using negative-ion electrospray ionization (ESI^-) mass spectrometry (ThermoFinnigan LCQ DECA ion trap mass spectrometer, San Jose, CA) as previously described (Wu et al., 2004). For the MS system, the heated capillary temperature was set at 200°C, spray voltage was 3.5 kV, and the sheath gas and auxiliary gas flow rate were 60 and 20 ml/min, respectively. All other parameters were set to the optimized conditions for ionization and detection of S4. Data acquisition was controlled by Xcalibur software (Revision B, ThermoQuest Corp., San Jose, CA). For MS^2 analysis, S4 or metabolite ions were isolated with a width of 1.5 m/z, and fragmented using a fragmentation energy ranging from 15 to 50%.

Biotinylation of the Hydrolysis Metabolites

The HPLC eluate from the first three minutes of the gradient run, as described above, was collected and concentrated under nitrogen. NHS-Biotin was dissolved in DMSO, and was added to the concentrated HPLC eluate (1:10/v:v) to a final concentration of 20 mM. The biotinylation reaction was conducted at room temperature for one hour. The reaction mixture was then centrifuged, and the supernatant was subjected to HPLC analysis using the same condition as described above.

Androgen Receptor Binding Assay

DMD Fast Forward. Published on November 4, 2005 as DOI: 10.1124/dmd.105.007112
This article has not been copyedited and formatted. The final version may differ from this version.

The binding affinity of the deacetylated metabolite, M1, was determined using cytosolic AR prepared from ventral prostates of castrated male Sprague-Dawley rats (about 250 g), as described previously (Mukherjee et al., 1996).

Transcriptional Activation Assay

The ability of the compounds to influence AR-mediated transcriptional activation was examined using a cotransfection system, as described previously (Yin et al., 2003b). Transcriptional activation by M1 was measured at multiple concentrations, ranging from 0.1 to 1000 nM, and was reported as a percentage of the transcriptional activation observed with 0.1 nM DHT. E_{max} and EC_{50} were determined by nonlinear regression analysis using WinNonlin and the Sigmoidal E_{max} model.

RESULTS

Identification of the Phase I Metabolites of S4

^{14}C-S4 (2 μM) was incubated with liver S9 at 37°C for two hours, and the ^{14}C-metabolites were separated on HPLC. The concentration was chosen according to the hepatic concentration of S4 at pharmacologically relevant doses as determined by total body autoradiography in rats (data not shown). Similar experiment was repeated using non-radiolabeled S4, and the fractions corresponding to the ^{14}C-metabolites were collected and subjected to MS analysis.

Four major metabolism pathways were identified (Figure 2 A): 1) deacetylation of the B-ring acetamide group; 2) hydrolysis of the amide bond; 3) reduction of the A-ring nitro group; and 4) oxidation of the B aromatic ring. Radiochromatographs corresponding to the identified metabolites are illustrated in Figure 2 B. MS^2 spectra and the proposed fragmentation pattern of S4 and its metabolites are shown in Figures 3, 4, and 6.

Deacetylation product M1, hydrolysis products M2, M2-OH and M3, and reduction product M4 were the major *in vitro* metabolites of S4 in liver S9 fractions. S4 and M1 shared very similar fragmentation pattern (Figure 3), except that the fragment ion at 150 *m/z* was not present in the M1 MS^2

spectrum due to the deacetylation of the B-ring acetamide group. A similar pattern was observed for M4 and M5 as well.

Besides these major metabolites, the corresponding oxidation products, S4-OH, M1-OH and M4-OH were also observed. As shown in Figure 2A and Figure 4 A through C, multiple oxidation products of S4 were identified, which could be due to differences in hydroxylation position on the B-ring. No A-ring hydroxylation product of S4 was observed. However, unlike S4, oxidation of M1 and M4 was only observed in the A-ring, not the B-ring. The fragmentation pattern of M1-OH and M4-OH changed dramatically as well, as shown in Figure 4 D and E. Also, two different M1 oxidation products were observed as separated by HPLC (Figure 2B). However, two products shared the same fragmentation pattern as shown in Figure 4D.

Among all the metabolites identified, the hydrolysis products were the most hydrophilic due to the presence of the carboxyl group, and most of them co-eluted with the solvent front (Figure 2B). M3, particularly, contains an amine group on the B-ring, which mimics the structure of an amino acid and makes the analysis of the metabolite more difficult. To facilitate the separation and detection of the molecule, we collected and concentrated the corresponding HPLC eluate, and modified the aromatic amine group. NHS-Biotin is a commonly used protein labeling reagent that specifically modifies primary amine groups (Figure 5A). Biotinylation of the B-ring amine group greatly facilitated the HPLC separation of the hydrolysis metabolites that contained the aromatic amine group, as shown in chromatogram in Figure 5B. On other hand, M3, the hydrolysis product with intact acetamide group on the B-ring, was not modified, and still co-eluted with the solvent front. The MS^2 fragmentation patterns for M3, M3-OH, and the biotinylated metabolite of M2 are shown in Figure 6.

Although M3 can not be modified, acidic condition could decrease the ionization of the carboxyl group and increase its retention time on column, while the hydrolysis products with the amine group would be highly ionized and eluted with the solvent front. The HPLC elution (first three minutes) containing M3, as separated under neutral pH (as described above), was collected and concentrated under

nitrogen. M3 was further separated from the solvent front using similar HPLC condition with pH 4.0 (0.2 % acetic acid), and was eluted at 15 minute (data not shown).

Comparison of the Phase I Metabolites of S4 in Different Species

The metabolic profile of S4 in different species was estimated and compared using human, rat, and dog liver S9 fraction. Similar total protein concentration (2 mg/ml) was used for all reactions. The relative abundance of each fraction in different reaction mixtures is presented in Figure 7A as a percentage of ^{14}C-S4 metabolized. Similarly; all four metabolic pathways were observed in the species tested. After two hour incubation, the predominant metabolite, M1, accounted for 61%, 44%, and 58% of the S4 metabolized in human, rat and dog S9 fraction, respectively. However, the relative contribution of other pathway was quite different in these three species.

In human S9 fraction, besides deacetylation, the other three metabolic pathways contributed very similarly to the metabolism of S4, with hydrolysis, reduction, and oxidation accounting for 11%, 16%, and 12% of S4 metabolized, respectively. However, reduction of S4 in human liver S9 fraction contributed to a relatively larger extent in S4 metabolism (16%), compared to those observed in rat (7%) and dog (2%) S9 fractions.

On the other hand, hydrolysis seemed to play a larger role in S4 metabolism by rat S9 fraction, accounting for 27% of the S4 metabolized, as compared to 11% and 14% in human and dog S9 fractions. More interestingly, M3 was the only hydrolysis product observed in rat S9 fraction, while the hydrolysis products by human and dog S9 fractions contained M2, M3, and their oxidized products, which indicated that hydrolysis might be a faster process than deacetylation or oxidation in rat S9 fraction.

Also, oxidation of S4 and M1 accounted for more than 20% of S4 metabolized by rat and dog S9 fractions, but only 12% of S4 metabolized by human S9 fraction. Considering the fact that more oxidized hydrolysis metabolites were observed in dog S9 fraction incubations compared to rat S9 fraction, oxidation might contribute more significantly to S4 metabolism in dog S9 fraction.

DMD Fast Forward. Published on November 4, 2005 as DOI: 10.1124/dmd.105.007112
This article has not been copyedited and formatted. The final version may differ from this version.

In general, the major metabolic pathways observed in three species tested were similar: deacetylation product M1 was the primary phase I metabolite of S4, with hydrolysis, reduction, and oxidation products observed in all three species as well.

Comparison of the Phase I Metabolism of S4 in Different Subcellular Fractions

The phase I metabolism of S4 was further estimated in incubations with different subcellular fractions of human liver preparations, including pooled human liver microsomes (HLM) and human liver cytosol. After two hour incubation, the metabolic profiles of S4 after incubation with HLM and human liver cytosol fractions were dramatically different (Figure 7B). As the majority of the phase I enzymes are located in HLM, the metabolic profile observed in the reactions with HLM was very similar to that observed with human liver S9 fraction (Figure 7A), as described above. However, in the presence of human liver cytosol, deacetylation product M1, was no longer the primary metabolite observed, accounting for only 16% of S4 metabolized; compared to 53% as observed in HLM incubations. On the contrary, reduction product M4 counted for more than 50% of S4 metabolized by human liver cytosol, compared to 11% as observed in HLM incubations.

Although the amide bond hydrolysis reaction was commonly believed to be catalyzed by esterase present in the cytosolic fraction, hydrolysis of S4 seemed to contribute to S4 metabolism by HLM to a much larger extent, 20%, as compared to 9% by the cytosolic fraction. Also, since the deacetylation reaction was preferred in the microsomal fraction, M3 turned out to be the major hydrolysis product in human liver cytosol incubates; while both acetylated (M3) and deacetylated hydrolysis products (M2 and M2-OH) of similar amount were observed in HLM incubates.

To further identify the major CYP enzymes responsible for phase I metabolism of S4, five major human CYP enzymes, including CYPs 1A2, 2C9, 2C19, 2D6, and 3A4, were tested by measuring the disappearance of S4 after 2 hour incubation with S4 (2 μM) at 37ºC. Among the five enzymes tested, CYP3A4 was identified as one of the major CYP enzymes that might be responsible for S4 metabolism at 2 μM (data not shown). When incubated with ^{14}C-S4 (2 μM), the metabolic profile of S4 by CYP3A4 was similar to that observed after incubation with HLM (Figure 7B). Recombinant human CYP3A4 mainly

DMD Fast Forward. Published on November 4, 2005 as DOI: 10.1124/dmd.105.007112
This article has not been copyedited and formatted. The final version may differ from this version.

catalyzed deacetylation, hydrolysis, and oxidation reactions, which accounted for 43%, 30%, and 24%, respectively, of S4 metabolized. No significant metabolism of S4 was observed after incubation with insect cell control microsome, which does not contain the recombinant CYP enzymes.

Kinetics of S4 Metabolism by Recombinant Human CYP3A4

The disappearance of S4 was determined as an initial measure to estimate the enzyme kinetics parameters of CYP3A4 (Figure 7). S4 showed similar affinity to CYP3A4 (16.1 μM) as testosterone (13 μM), but a lower Vmax (1.6 pmole/(pmole*min)) compared to testosterone (7.6 pmole/(pmole*min), data not shown).

Characterization of M1 as an Active Metabolite of S4

S4 deacetylation product M1 maintained the core structure of the pharmacophore, which suggests that it could also interact with AR and act as an active metabolite. We previously showed that other B-ring amine derivatives showed moderate binding affinity towards AR (Yin et al., 2003b). *In vitro* receptor binding assay showed that M1 bound the AR with relatively lower affinity (Ki, 24.6 nM) compared to S4 (Ki, 4.0 nM). Furthermore, it behaved as a partial agonist in an *in vitro* transcriptional activation assay (Figure 9), with relative agonist activity of 42 % at 1 μM, compared to 0.1 nM DHT. These results suggested that M1 could also activate AR and might contribute to the pharmacological activity of S4 *in vivo*. More detailed studies of M1 are reported separately.

DISCUSSION

The major phase I metabolism pathways of S4 in rats, dogs, and humans, were identified using different liver enzyme preparations: including deacetylation of the B-ring acetamide group, hydrolysis of the amide bond, reduction of the A-ring nitro group, and oxidation of the aromatic rings. Compared to our previous compound, acetothiolutamide, the introduction of the ether linkage in S4 eliminated the oxidation of the previous thio-ether linkage and reduced oxidation of the B-ring. However, it also decreased the overall stability of the amide bond, which was susceptible to extensive hydrolysis, particularly in rat. The cyano group on the A-ring was replaced by the nitro group in S4, considering the

fact that nitro group might improve the binding affinity of the ligand to AR, as shown in our previous study (Yin et al., 2003b). However, the nitro group was susceptible to reduction, which made the A-ring a metabolically labile site as well. Similar to acetothiolutamide, deacetylation of the B-ring acetamide group continue to play prominent role in S4 metabolism.

Based on the structure-activity relationship established in our previous studies (He et al., 2002; Yin et al., 2003b), the introduction of the ether linkage and/or the acetamide substitution on the para-position of B-ring was crucial to the agonist activity of this class of ligands. The ether linkage, particularly, is required for the high binding affinity of the ligand to AR. Therefore, modification of other metabolically labile sites would be necessary to improve the metabolic stability of the compound while maintaining its agonist activity: 1) nitro substitution on the A-ring can be replaced by cyano group; 2) acetamide group on the B-ring can be substituted by halogens, like compound S1, as presented in our previous pharmacologic study (Yin et al., 2003a), which will not only avoid the deacetylation reaction, but also reduce B-ring oxidation by reducing its electron density, since halogens are stronger electron withdrawn groups.

Although the precise mechanisms by which the ether linkage improves the agonist activity of the ligand but decreases the metabolic stability of the amide bond is unclear, recently solved bicalutamide bound AR LBD mutant (T741L) crystal structure (Bohl et al., 2005) suggested that an intra-molecular hydrogen bond between the oxygen atom from the ether linkage and the hydrogen atom from the amide bond might be related to the susceptibility of the amide bond to hydrolysis. Further, the electron density of the oxygen atom is greatly affected by the para-substituents on the B-ring, suggesting that compounds incorporating different para-substituents might show differing degree of hydrolysis. In the case of bicalutamide, the oxygen atom from the sulfonyl linkage could also form a similar intra-molecular hydrogen bond, which could be related to the extensive hydrolysis of its amide bond in human. However, this hypothesis needs to be further confirmed by more detailed studies using structural analogs containing different B-ring substitutions. Nevertheless, S4 appeared to undergo more extensive amide bond hydrolysis in rat liver S9 fraction than in human liver S9 fraction (Figure 7A), suggesting that amide bond

hydrolysis might not be the major metabolic pathway in human as compared to in rat, similar to bicalutamide.

On the other hand, S4 metabolism profiles in three different species were characterized and compared. Since the *in vitro* incubation was carried out for two hours due to the low specific activity of the ^{14}C-S4, the reported data only represented the 'estimates' of relative rates of metabolism via different pathways and fractions. Among all three species tested, deacetylation accounted for about half of the S4 metabolized *in vitro*, and is likely the major metabolic pathway *in vivo*. Furthermore, the deacetylated metabolite M1 bound to AR and initiate transcription activation *in vitro*, suggesting that it might contribute to the *in vivo* pharmacologic activity of S4 as well. Additional pharmacokinetic studies to examine the disposition of M1 are necessary to determine the *in vivo* activity of M1 as active metabolite.

Amide bond hydrolysis and acetamide deacetylation occurred in both cytosolic and microsomal fractions of human liver preparation (Figure 7B). The cytosolic enzymes mainly catalyzed the hydrolysis reaction, while the microsomal enzymes primarily catalyzed the deacetylation reactions, which suggested that the microsomal CYP enzymes might also be responsible for the hydrolysis and deacetylation of S4. CYP3A4 is responsible for the metabolism of more than 70% of marketed drugs (Casarett et al., 1996), with oxidation being the most common metabolic reaction. Similarly, CYP3A4 is responsible for the oxidation of S4 *in vitro*, and even bicalutamide oxidation in human, as recently described by Cockshott (Cockshott, 2004). However, in our study, human CYP3A4 appeared to be able to catalyze hydrolysis reactions as well. CYP3A4 catalyzed hydrolysis reactions were rarely documented (Ji et al., 2004), however, it does exist. As described above (Figure 7B), in the presence of NADPH, CYP3A4 could not only catalyze the oxidation of S4, but also catalyzed the hydrolysis of the amide bond and deacetylation of the acetamide group on the B-ring. The deacetylation reaction can also be considered as a hydrolysis reaction. Also, kinetics studies showed that S4 had similar affinity (K_m) to CYP3A4 as testosterone (Figure 8). At pharmacologically relevant concentrations, it is likely that CYP3A4 would be responsible for the deacetylation of S4 in human.

Besides the identification of the major *in vitro* metabolites of S4 in three different species, the HPLC separation and MS analysis of the hydrolysis products, M2 and M3, were also a challenging part of our study. The presence of both carboxyl and amine groups in M2 made this molecule extremely hydrophilic. Similar to amino acids, M2 could not be separated from the solvent front under either acidic or basic conditions as we tested, which is much different from M3. The intact acetamide group in M3 made it easier to separate under acidic conditions (pH 4.0). To facilitate the separation without using stringent condition in sample preparation and/or separation, we used a derivatization method that is often used in amino acid analysis. NHS-Biotin is one of the most commonly used protein labeling reagent that specifically modifies primary amine groups. The aromatic amine group in M2 could serve as a perfect substrate for similar modification. The addition of the large biotin moiety could not only increase the column retention time of the molecule, but also increase the ionization efficiency during MS analysis. The mild reaction condition (room temperature, neutral pH) excluded the possible hydrolysis due to artificial effects (i.e., strong acidic condition). As shown in Figure 5B, both M2 and M2-OH were modified and separated successfully from the void peak. This design might provide a unique strategy for analyzing highly hydrophilic metabolites that contain primary amine groups.

Besides the differences observed in the phase I metabolism of S4, potential species differences in the phase II metabolizing enzymes might also play a role in the *in vivo* metabolism of S4. As discussed above, the aromatic amine group in M1 and M2 is susceptible to modification; it might also be acetylated again by phase II enzyme, like N-acetyl transferase (NAT), and be converted to S4. The interaction between M1 and NAT, and potential species difference in S4 metabolism was studied in more detail in separate studies.

For the other hydrolysis product M3, although it was easier to separate under acidic condition (pH 4.0), the acidic condition is generally not recommended for the MS analysis with negative ion mode. However, our previous study (Wu et al., 2004) has shown that lower concentrations of acetic acid can actually improve the MS response of S4 under negative ion mode. Similarly, the presence of 0.2 % acetic

acid during MS analysis didn't suppress the MS response of M3 in this study, which further confirmed that mild acidic condition could be used under negative ion mode as well.

In summary, *in vitro* metabolism studies showed that S4 was mainly metabolized by deacetylation of the B-ring acetamide group, hydrolysis of the amide bond, and reduction of the A-ring nitro group, with deacetylation being the major pathway in all three species tested, while amide bond hydrolysis more significant in rat than in human and dog.

REFERENCES

Bohl CE, Gao W, Miller DD, Bell CE and Dalton JT (2005) Structural basis for antagonism and resistance of bicalutamide in prostate cancer. *Proc Natl Acad Sci U S A* **102**:6201-6206.

Boyle GW, McKillop D, Phillips PJ, Harding JR, Pickford R and McCormick AD (1993) Metabolism of Casodex in laboratory animals. *Xenobiotica* **23**:781-798.

Casarett LJ, Klaassen CD, Amdur MO and Doull J (1996) *Casarett and Doull's toxicology: the basic science of poisons*. McGraw-Hill Health Professions Division, New York.

Cockshott ID (2004) Bicalutamide: clinical pharmacokinetics and metabolism. *Clin Pharmacokinet* **43**:855-878.

Dalton JT, Mukherjee A, Zhu Z, Kirkovsky L and Miller DD (1998) Discovery of nonsteroidal androgens. *Biochem Biophys Res Commun* **244**:1-4.

Gao W, Kearbey JD, Nair VA, Chung K, Parlow AF, Miller DD and Dalton JT (2004) Comparison of the Pharmacological Effects of a Novel Selective Androgen Receptor Modulator (SARM), the 5{alpha}-Reductase Inhibitor Finasteride, and the Antiandrogen Hydroxyflutamide in Intact Rats: New Approach for Benign Prostate Hyperplasia (BPH). *Endocrinology* **145**:5420-5428.

He Y, Yin D, Perera M, Kirkovsky L, Stourman N, Li W, Dalton JT and Miller DD (2002) Novel nonsteroidal ligands with high binding affinity and potent functional activity for the androgen receptor. *Eur J Med Chem* **37**:619-634.

Ji HY, Lee SS, Yoo SE, Kim H, Lee DH, Lim H and Lee HS (2004) In vitro metabolism of a new neuroprotective agent, KR-31543 in the human liver microsomes: identification of human cytochrome P450. *Arch Pharm Res* **27**:239-245.

Katchen B and Buxbaum S (1975) Disposition of a new, nonsteroid, antiandrogen, alpha,alpha,alpha-trifluoro-2-methyl-4'-nitro-m-propionotoluidide (Flutamide), in men following a single oral 200 mg dose. *J Clin Endocrinol Metab* **41**:373-379.

Kearbey JD, Wu D, Gao W, Miller DD and Dalton JT (2004) Pharmacokinetics of S-3-(4-acetylamino-phenoxy)-2-hydroxy-2-methyl-N-(4-nitro-3-trifluoromethyl-phenyl)-propionamide in rats, a nonsteroidal selective androgen receptor modulator. *Xenobiotica* **34**:273-280.

McKillop D, Boyle GW, Cockshott ID, Jones DC, Phillips PJ and Yates RA (1993) Metabolism and enantioselective pharmacokinetics of Casodex in man. *Xenobiotica* **23**:1241-1253.

Mukherjee A, Kirkovsky L, Yao XT, Yates RC, Miller DD and Dalton JT (1996) Enantioselective binding of Casodex to the androgen receptor. *Xenobiotica* **26**:117-122.

Negro-Vilar A (1999) Selective androgen receptor modulators (SARMs): a novel approach to androgen therapy for the new millennium. *J Clin Endocrinol Metab* **84**:3459-3462.

Wu Z, Gao W, Phelps MA, Wu D, Miller DD and Dalton JT (2004) Favorable effects of weak acids on negative-ion electrospray ionization mass spectrometry. *Anal Chem* **76**:839-847.

Yin D, Gao W, Kearbey JD, Xu H, Chung K, He Y, Marhefka CA, Veverka KA, Miller DD and Dalton JT (2003a) Pharmacodynamics of selective androgen receptor modulators. *J Pharmacol Exp Ther* **304**:1334-1340.

Yin D, He Y, Perera MA, Hong SS, Marhefka C, Stourman N, Kirkovsky L, Miller DD and Dalton JT (2003b) Key structural features of nonsteroidal ligands for binding and activation of the androgen receptor. *Mol Pharmacol* **63**:211-223.

Yin D, Xu H, He Y, Kirkovsky LI, Miller DD and Dalton JT (2003c) Pharmacology, pharmacokinetics, and metabolism of acetothiolutamide, a novel nonsteroidal agonist for the androgen receptor. *J Pharmacol Exp Ther* **304**:1323-1333.

FOOTNOTES:

Financial support:

These studies were supported by grants from GTx Inc. (Memphis, TN) and the National Institute of Diabetes and Digestive and Kidney Diseases (R01 DK59800) to J.T.D. and D.D.M.

Financial interest:

J.T.Dalton and D.D.Miller are employees of GTx, Inc.

Send reprint requests to:

James T. Dalton, Ph.D., 500 West 12th Avenue, L.M. Parks Hall, Room 242, Columbus, OH 43210. E-mail: DALTON.1@OSU.EDU

LEGENDS FOR FIGURES

Figure 1. Phase I metabolism of Flutamide (A) (Katchen and Buxbaum, 1975) and bicalutamide (B) (Boyle et al., 1993; McKillop et al., 1993).

Figure 2. Summary of phase I metabolism pathway of S4. A. Phase I metabolism pathways of ^{14}C-S4 (uniformly labeled B-ring) as determined in human, rat, and dog liver preparations. B. Radiochromatogram displaying the metabolism of ^{14}C-S4 by pooled human liver S9 fraction.

Figure 3. MS^2 spectra (ESI negative ion mode) of S4 and the reduction and deacetylation products M1, M4, and M5.

Figure 4. MS^2 spectra (ESI negative ion mode) of the oxidation products S4-OH, M1-OH, and M4-OH. Three different S4 oxidation metabolites with different fragmentation patterns (A, B, C) were identified.

Figure 5. Derivatization and separation of M2. A. Biotinylation reaction of S4 by NHS-Biotin. B. Radiochromatogram displaying the separation of biotinylated ^{14}C-M2 and ^{14}C-M2-OH from ^{14}C-M3.

Figure 6. MS^2 spectra (ESI negative ion mode) of the amide bond hydrolysis products M3, M3-OH, and the biotinylated M2 and M2-OH (B, C).

Figure 7. The relative abundance of the major *in vitro* metabolites of ^{14}C-S4 after incubation with different liver enzyme preparations. A. Metabolic profile of ^{14}C-S4 in the presence of human, rat, and dog liver S9 fractions. B. Metabolic profile of ^{14}C-S4 in the presence of different subcellular fractions of

human liver. The reaction was carried out in the presence of different liver enzyme preparations for 2 hours at 37ºC.

Figure 8. Enzyme kinetics of S4 metabolism by CYP3A4 as determined by measuring the disappearance of S4. The reaction was carried out in the presence of 200 pmole/ml CYP3A4 for 10 minutes at 37ºC.

Figure 9. *In vitro* AR transcriptional activation by M1 using co-tranfection assay. The activation by M1 was presented as a percentage of the activation obtained in the presence of 0.1 nM DHT.

DMD Fast Forward. Published on November 4, 2005 as DOI: 10.1124/dmd.105.007112
This article has not been copyedited and formatted. The final version may differ from this version.

A. Flutamide

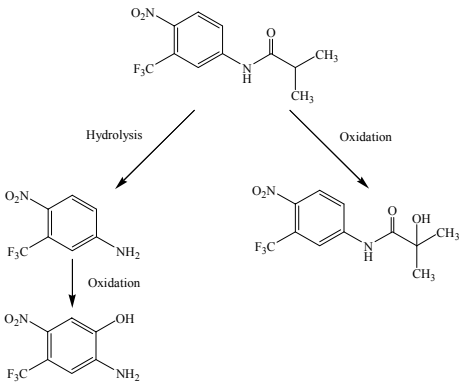

B. Bicalutamide

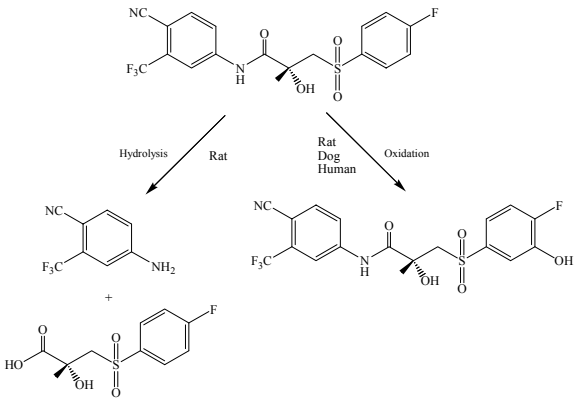

Figure 1

DMD Fast Forward. Published on November 4, 2005 as DOI: 10.1124/dmd.105.007112
This article has not been copyedited and formatted. The final version may differ from this version.

A.

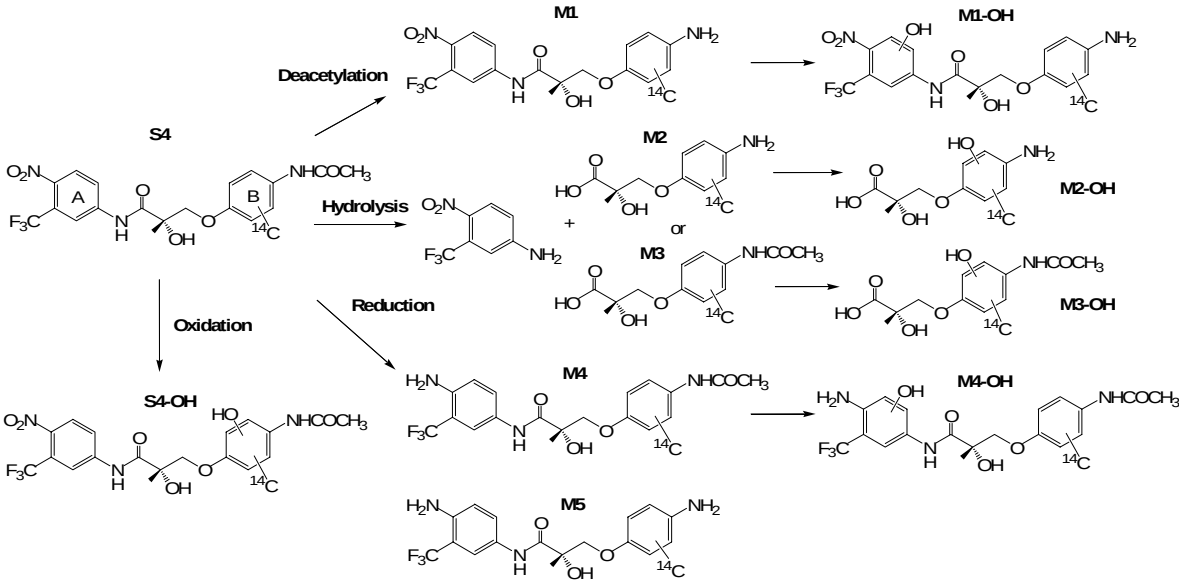

B.

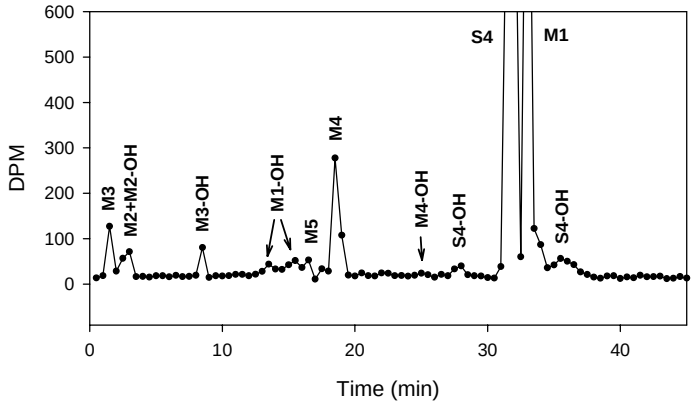

Figure 2

DMD Fast Forward. Published on November 4, 2005 as DOI: 10.1124/dmd.105.007112
This article has not been copyedited and formatted. The final version may differ from this version.

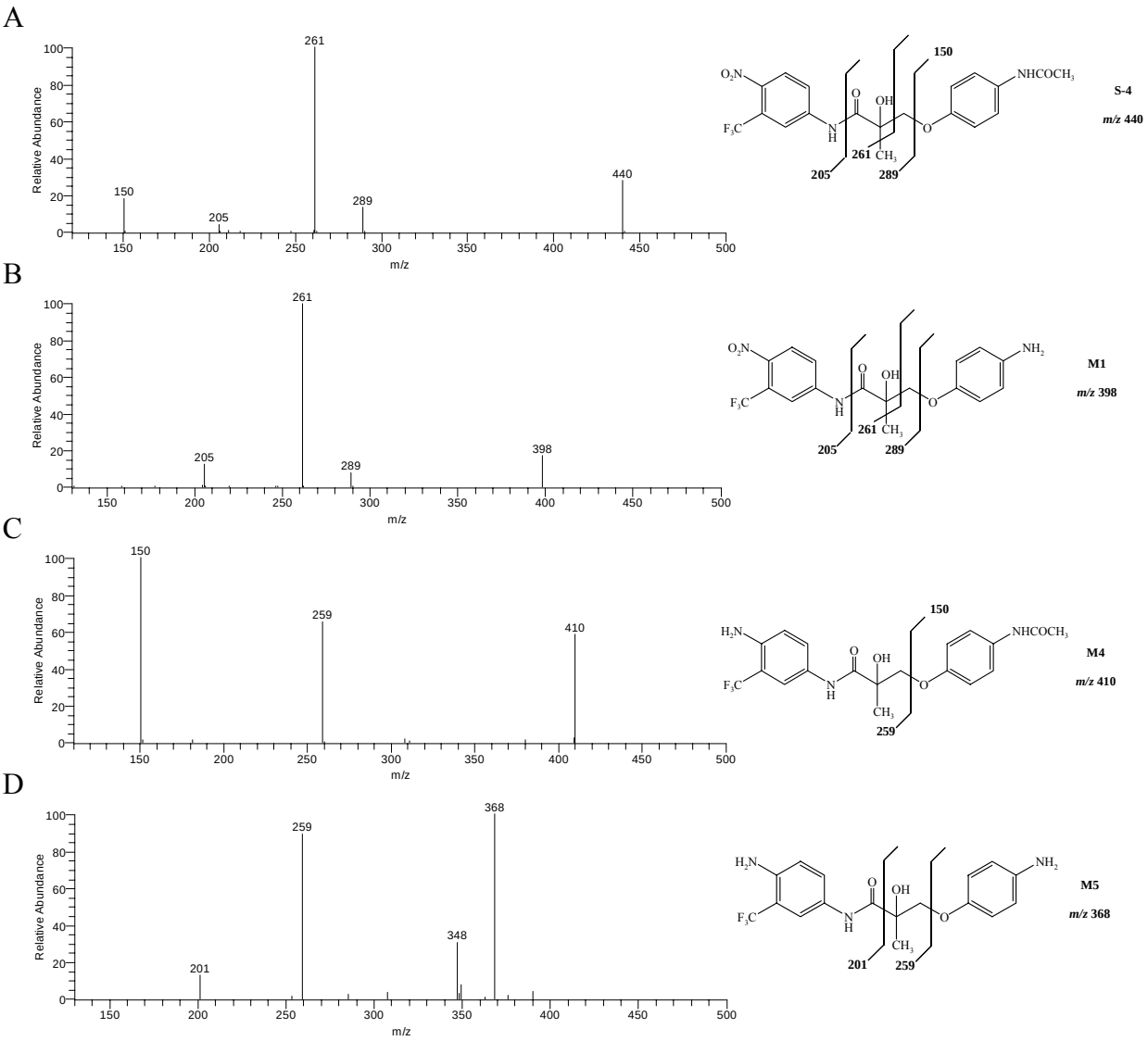

Figure 3

DMD Fast Forward. Published on November 4, 2005 as DOI: 10.1124/dmd.105.007112
This article has not been copyedited and formatted. The final version may differ from this version.

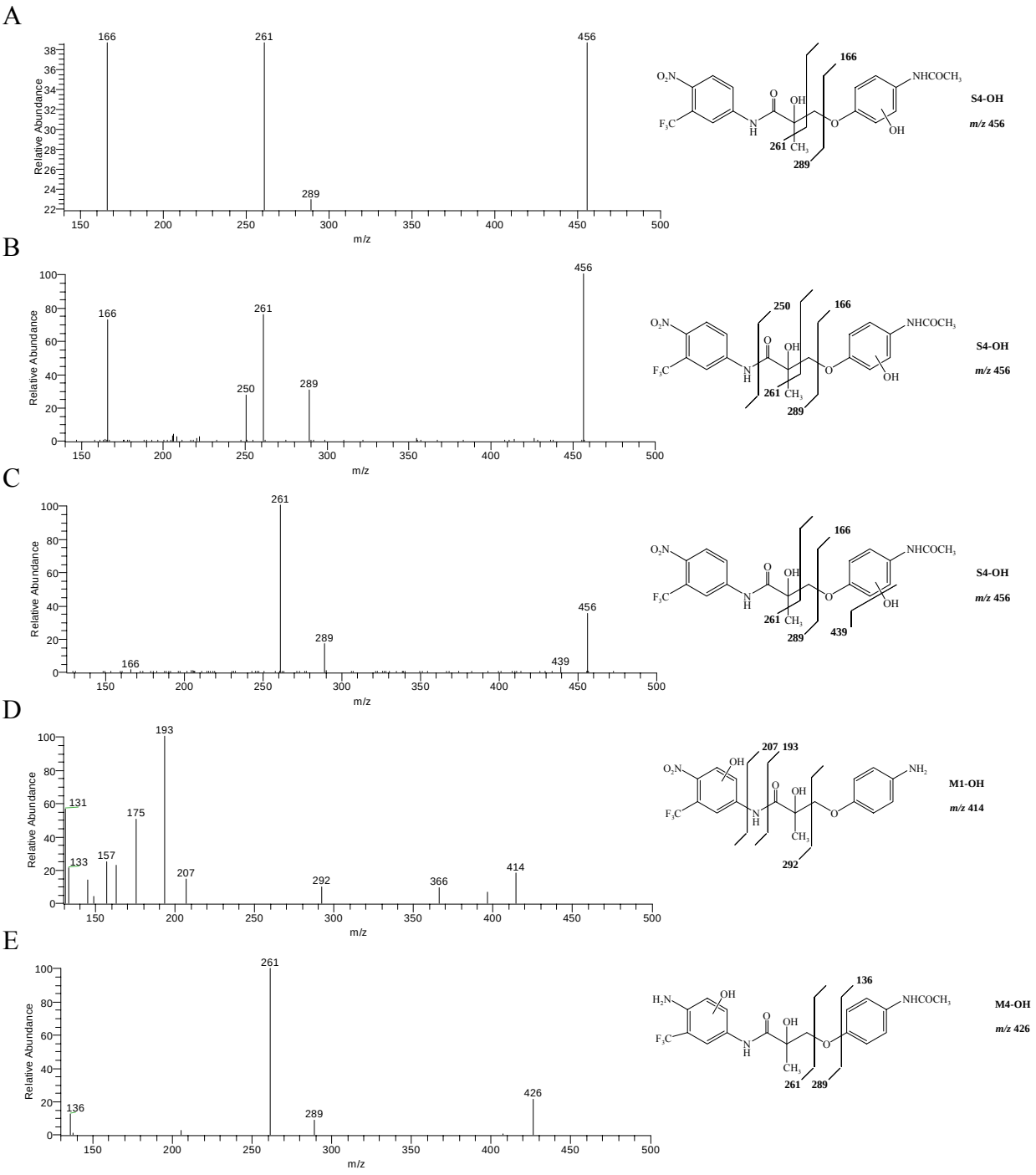

Figure 4

DMD Fast Forward. Published on November 4, 2005 as DOI: 10.1124/dmd.105.007112
This article has not been copyedited and formatted. The final version may differ from this version.

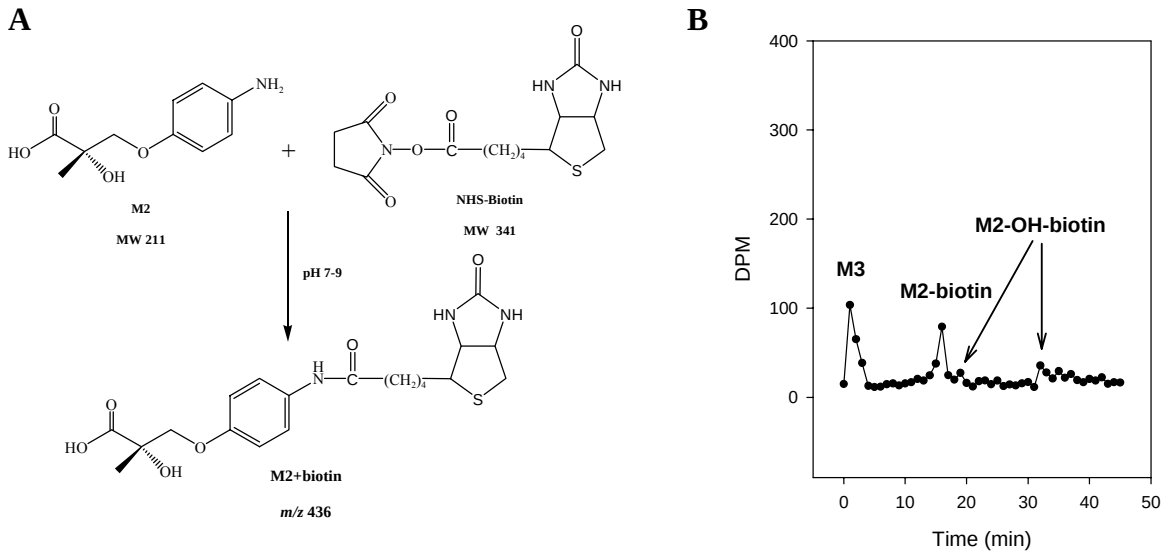

Figure 5

DMD Fast Forward. Published on November 4, 2005 as DOI: 10.1124/dmd.105.007112
This article has not been copyedited and formatted. The final version may differ from this version.

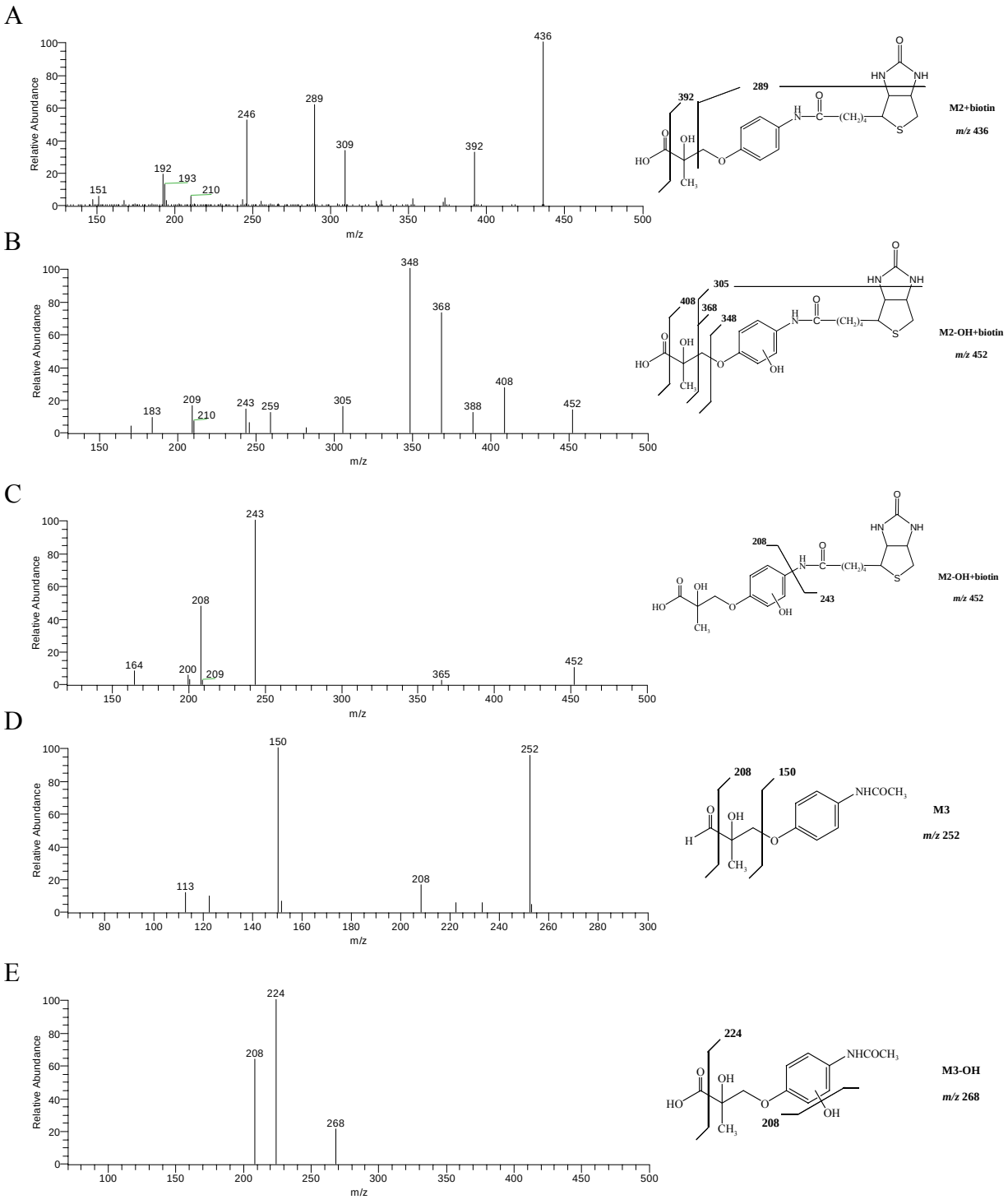

Figure 6

DMD Fast Forward. Published on November 4, 2005 as DOI: 10.1124/dmd.105.007112
This article has not been copyedited and formatted. The final version may differ from this version.

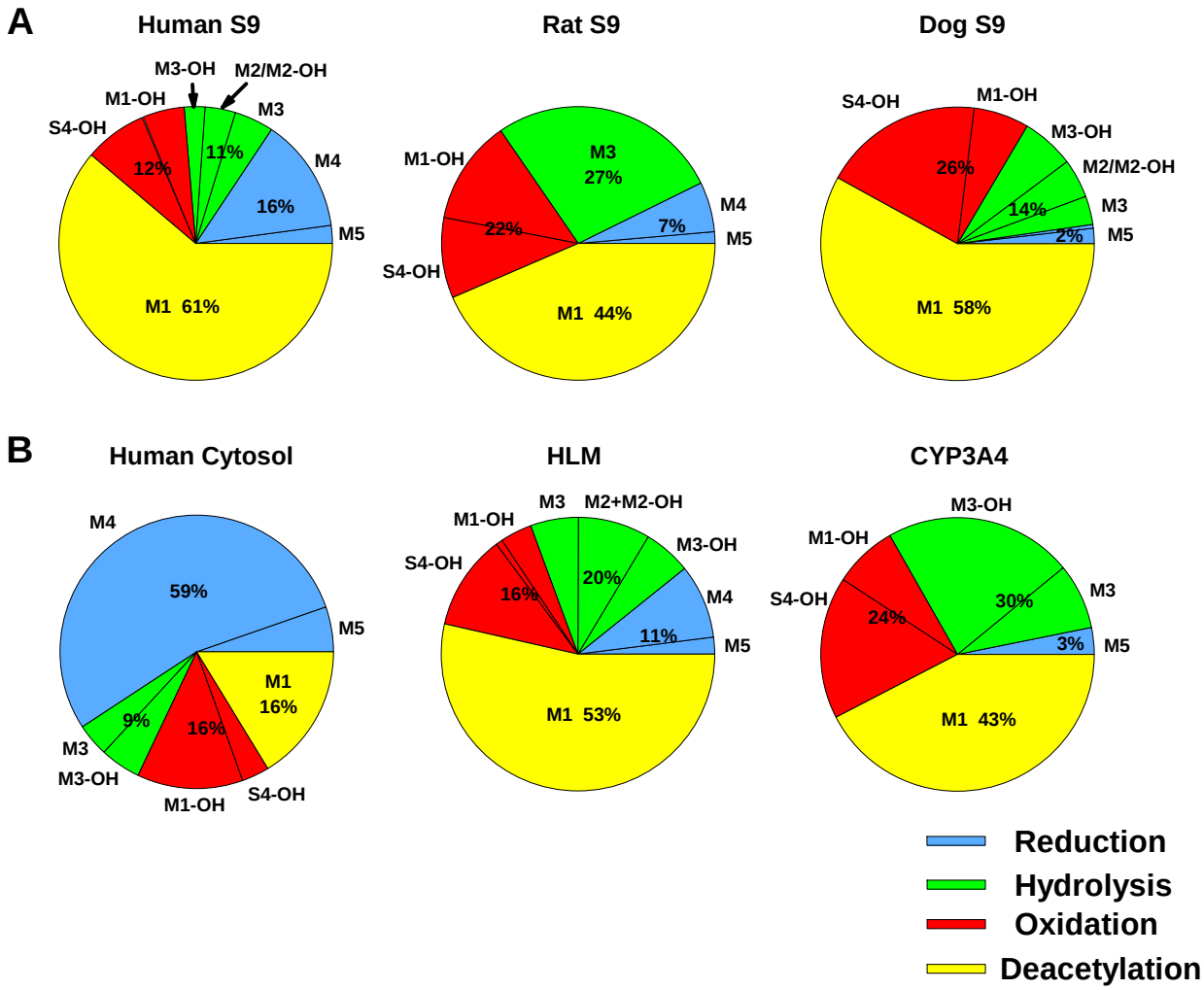

Figure 7

DMD Fast Forward. Published on November 4, 2005 as DOI: 10.1124/dmd.105.007112
This article has not been copyedited and formatted. The final version may differ from this version.

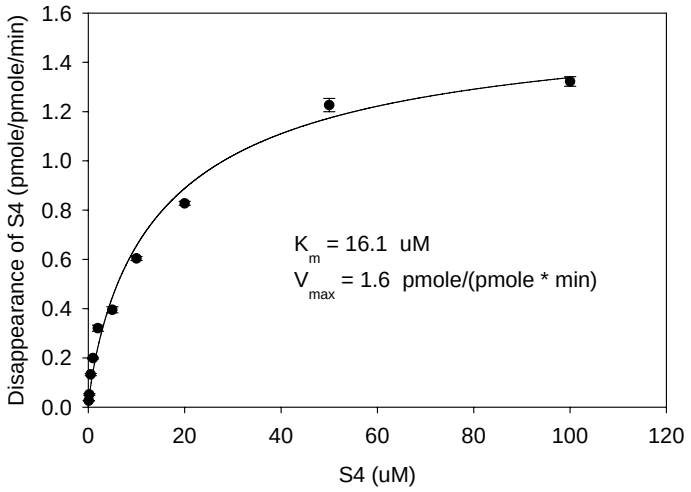

Figure 8

DMD Fast Forward. Published on November 4, 2005 as DOI: 10.1124/dmd.105.007112
This article has not been copyedited and formatted. The final version may differ from this version.

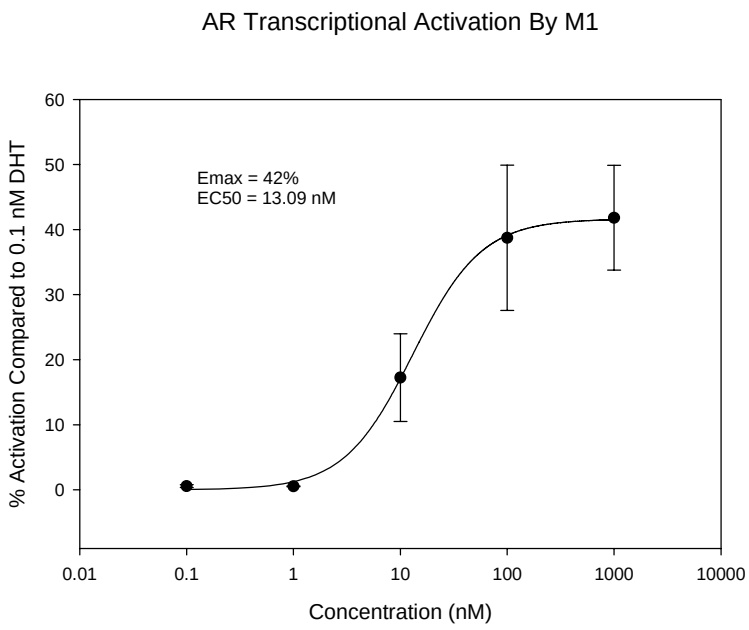

Figure 9